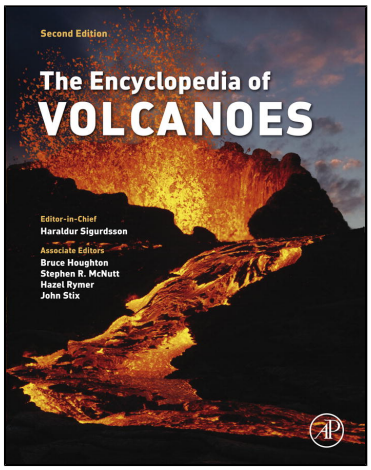

From Cioni, R., Pistolesi, M., Rosi, M., 2015. Plinian and Subplinian Eruptions. In: Sigurdsson, H., Houghton, B., Rymer, H., Stix, J., McNutt, S. (Eds.), The Encyclopedia of Volcanoes, pp. 519–535.
ISBN: 9780123859389

Academic Press

Chapter 29

Plinian and Subplinian Eruptions

Raffaello Cioni and Marco Pistolesi
Dipartimento di Scienze della Terra, via G. La Pira, Firenze, Italy

Mauro Rosi
Dipartimento Protezione Civile, via Vitorchiano, Roma, Italy

Chapter Outline

GLOSSARY

ash Pyroclastic fragments finer than 2 mm. A further distinction can be made between coarse (2 mm−63 μm) and fine (finer than 63 μm) ash.

ballistic clasts Decimetric to metric clasts ejected from the vent, whose size was too large to be entrained into the vertical jet of the eruptive plume. **Ballistic clasts** are ejected with an important horizontal component of velocity.

co-PDC ash Fine ash deposit resulting from the delayed sedimentation of an ash-rich, convective plume formed by the buoyant detachment of a gas−ash mixture from the top of a pyroclastic density current (PDC). In presence of wind, co-PDC ash settles far away from the PDC deposit.

co-plinian ash The coarse and fine ash related to delayed sedimentation from the umbrella region. Well identifiable as a normally graded bed at the top of the proximal and medial plinian fallout deposits from eruptions under no-wind conditions.

eruption intensity (*I*) An index related to mass discharge rate (MDR, in kg/s) and eruption column height. Calculated as $I = \log_{10}(\text{MDR}) - 3$.

eruptive plume A general term indicating the convective region of the eruptive column.

isopach Line connecting points of equal deposit thickness.

isopleth Line connecting points of equal value for particle size, e.g. diameter of maximum lithic clasts.

juvenile clasts Fragments derived from the explosive disruption of the erupting magma.

magma chamber A shallow reservoir in which magma coming from the source region may accumulate and evolve before erupting. Magma chamber shape can be largely variable, from tabular bodies (dyke, sills) to more sub-equant shapes (laccoliths, plutons).

magnitude An index related to the mass (kg) erupted during an eruption. Magnitude (M) scale is calculated as $M = \log_{10}(\text{erupted mass}) - 7$.

mass discharge rate Mass eruption rate (kg/s). Mass discharge rate (MDR) scales directly (approximately as the fourth root) to the total height reached by the eruptive column.

phreatomagmatic activity Activity related to the involvement of external water during an eruption, by direct contact with the ascending magma. The more general term hydromagmatic activity is used here to describe the interaction with either groundwater or surface water bodies (sea, lake).

pyroclastic density current (PDC) Gas−pyroclast mixture flowing along the ground and driven by the density contrast (negative buoyancy) with the surrounding fluid (atmosphere, water). PDCs can be generated by various eruptive processes: eruption column collapse, lateral explosions or landslides of hot material, such as a lava dome.

volcanic explosivity index (VEI) A scale for the explosive phases of an eruption, mainly based on the column height or on the mass

The Encyclopedia of Volcanoes. http://dx.doi.org/10.1016/B978-0-12-385938-9.00029-8

The Encyclopedia of Volcanoes, Second Edition, 2015, 519−535

ejected as pyroclasts. It relies on the assumption of a direct proportionality between magnitude and intensity of an eruption, and, as first introduced, varied from 0 to 8. The use of a negative VEI has been proposed to describe small-scale, mainly basaltic, eruptions.

wall-rock lithic clasts Clasts derived from the fragmentation of rocks from the nonvolcanic basement (accidental lithics), or comagmatic rocks emplaced during preceding eruptions (accessory or cognate lithics).

1. INTRODUCTION

In modern volcanology, the term "plinian" encompasses explosive eruptions characterized by the quasi-steady, hours-long, high-speed discharge into the atmosphere of a high-temperature, multiphase mixture (gas, solid, and liquid particles), forming a buoyant vertical column that reaches heights of tens of kilometers (Figure 29.1(A)). After having attained its maximum height, the column eventually spreads laterally into an "umbrella" cloud (Figure 29.1(A) and (C)), which maintains its identity for hundreds of kilometers. Conversely, when buoyancy of the erupting mixture is not achieved, the basal part of the column collapses and forms a sustained, ground-hugging cloud of hot gases and pyroclasts, which disperse around the volcano (Figures 29.1(B) and (D)).

The volcanic phenomenon was superbly described for the first time in two letters written by Pliny the Younger to Tacitus to report on his uncle's death during the eruption of Vesuvius (Italy) in AD 79. Pliny's description of the eruptive cloud as a pine tree with a high vertical trunk enlarging into several branches is fully evocative of the actual phenomenon.

I cannot give you a more exact description of its appearance than by comparing to a pine tree; for it shot up to a great height in the form of a tall trunk, which spread out at the top as though into branches. ... Occasionally it was brighter, occasionally darker and spotted, as it was either more or less filled with earth and cinders.

Plinian columns disperse large quantities of highly vesicular pyroclastic material, which settles to the ground over vast areas as a continuous shower. Resulting deposits consist of blankets of coarse-grained, well-sorted pumice in the proximal area, grading downwind to widely dispersed **ash** beds.

Although plinian eruptions by definition include a sustained phase, they typically consist of a complex succession of volcanic pulses. These may include sustained, quasi-steady convective plumes that alternate and overlap with pulsatory explosions of different style, intensity, and dynamics (from vulcanian explosions, to phases of prolonged ash emission, to **phreatomagmatic activity**, to the emission of lava flows or domes). As a result, simple classification schemes merely based on the dynamics and the products of the sustained phase are in some cases inadequate, as they ignore the complex time-evolution of

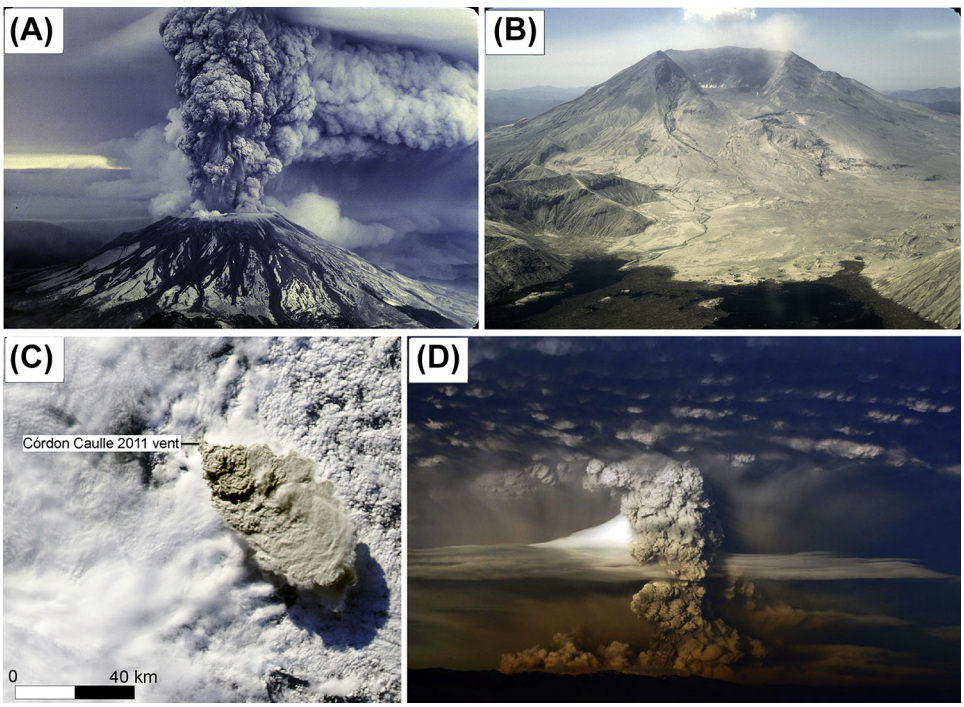

FIGURE 29.1 Eruption columns of plinian and suplinian eruptions. Mount St. Helens (USA) during (A) and immediately after (B) the 1980 eruption; (C) and (D) 2011 eruption of Puyehue-Córdon Caulle (Chile). Note in (D) contemporaneous convective and collapsing regimes with pyroclastic flow generation. *Photos (A) and (B) are by Richard G. Bowen, courtesy of the Bowen family. Picture (C) is courtesy of NASA.*

the eruption dynamics. From this perspective, a plinian eruption is more realistically described as a succession of different eruptive phases. In the following text, the term *plinian pulse* will be used to specifically address the sustained plinian part of more complex eruptive scenarios. For example, the dominant phase of a *plinian eruption* can consist of a combination of *plinian pulses*, whereas the onset can be represented by *vulcanian pulses*. The term *plinian regime* will be instead used as a more general term, to address the sustained high flow rate discharge of fragmented magma, which may either result in the formation of a convective column or of a collapsing cloud generating a **pyroclastic density current**.

The term *subplinian* was first introduced to describe eruptions of lower scale but dynamics similar to plinian events. The study of subplinian eruptions has revealed that an important distinguishing feature is the occurrence of high-frequency fluctuations or of temporary breaks in the discharge, with the repeated generation of short-lived convective plumes often alternated with phases of quiescence or of lower intensity, explosive or effusive activity.

All the eruptive events sharing a plinian regime have been often grouped under the general term of "plinian eruptions," which encompasses subplinian, plinian, and ultraplinian styles.

2. CLASSIFICATION ISSUES AND GENERAL CHARACTERISTICS

Explosive eruptions can be classified according to different criteria. Recent events at monitored volcanoes are classified by using ground-based geophysical data and satellite remote-sensing observations, as well as features of the tephra deposits. In contrast, past eruptions are classified solely on the basis of deposit features. These two different classification approaches have been analyzed and discussed by many authors with the aim of establishing a coherent classificatory grid (Walker, 1973; Pyle, 1989). However, the results of the two classification approaches are not fully tested for high intensity eruptions (with eruptive columns higher than 30 km), mainly due to the scarcity of observed cases. For this reason, it is still common practice to use deposit characteristics to classify high-intensity eruptions.

Volcanic Explosivity Index (VEI) values in the range of 4–6 characterize subplinian and plinian eruptions. Recurrence rates of about 10 plinian (VEI 5–6) and 30–40 subplinian (VEI 4) events per century strongly contrast with the very low recurrence rate of ultraplinian eruptions (VEI 7, less than 1 per 1000 years).

2.1. Plinian Eruptions

Plinian and ultraplinian eruptions share common eruption dynamics, but different values of **eruption intensity** and **magnitude** (10–12, and 4–8, respectively, according the scale of Pyle, 2000).

During plinian pulses, a mixture of gas and particles (juvenile, cognate, and lithic material) is discharged from a vent at high speed (typically 150–600 m/s). Variations in the discharge or in parameters controlling the eruption dynamics (e.g. magma composition, volatile content, vent and conduit geometry) generally occur over a time scale longer than the characteristic times of the different processes, which dominate magma ascent, magma fragmentation, and plume development. This results in a sustained, quasi-steady eruption column.

In the gas-thrust region, the eruptive jet incorporates air and eventually gains a positive buoyancy with respect to the ambient atmosphere (Figures 29.1(A)–(C)), shifting to a convective regime. Above the gas-thrust, the buoyant column rises in the atmosphere and reaches neutral buoyancy, then starts to propagate laterally as a radially spreading density current, advected by winds. Powerful eruption columns typically penetrate the local tropopause and spread into the stratosphere (Figure 29.2).

The volume of ejected material produced by individual plinian pulses ranges typically between 0.1 and 10 km^3, with peak **Mass Discharge Rates** (MDR) between 10^6–10^8 kg/s (Table 29.1). Due to the very high discharge rate, the duration of plinian pulses generally ranges between a few hours (3 h for the 1815 Tambora eruption, Sunda arc, Indonesia) to days (about 48 h for the 1991 Cerro Hudson eruption, Chile). Many plinian eruptions consist of repeated plinian pulses (at least three for the 1982 El Chichón eruption, Mexico, and for the 1912 Katmai eruption, Alaska), each separated by hiatuses of hours. Although considered quasi-steady, many plinian pulses show a progressive increase of MDR, which is recorded as inverse grading (coarsening upward) of the resulting fallout deposits.

In plinian and ultraplinian eruptions, interplay of the source parameters (exit velocity, MDR, magma gas content, total grain-size distribution, conduit geometry) has a fundamental role in determining the fate of the eruption column (Figure 29.3). Within the typical range of MDRs for the plinian regime, sustained, buoyant plumes may rapidly shift to collapsing behavior and generation of PDCs (Figure 29.1(D)). Consequently, fall and PDC deposits are commonly interbedded in plinian sequences. PDC deposits may represent only a small fraction of total erupted volume (<20% for the AD 79 Vesuvius eruption) or, conversely, the larger part (40% for 1912 Katmai eruption, to 60% for the Minoan eruption of Santorini, to 95% estimated for the 1815 Tambora eruption). The transition from sustained to collapsing conditions is generally preceded by a phase of column unsteadiness (Figure 29.3), during which partial collapse of the column produces pulsating, dilute PDCs (transitional regime; Neri et al., 2002).

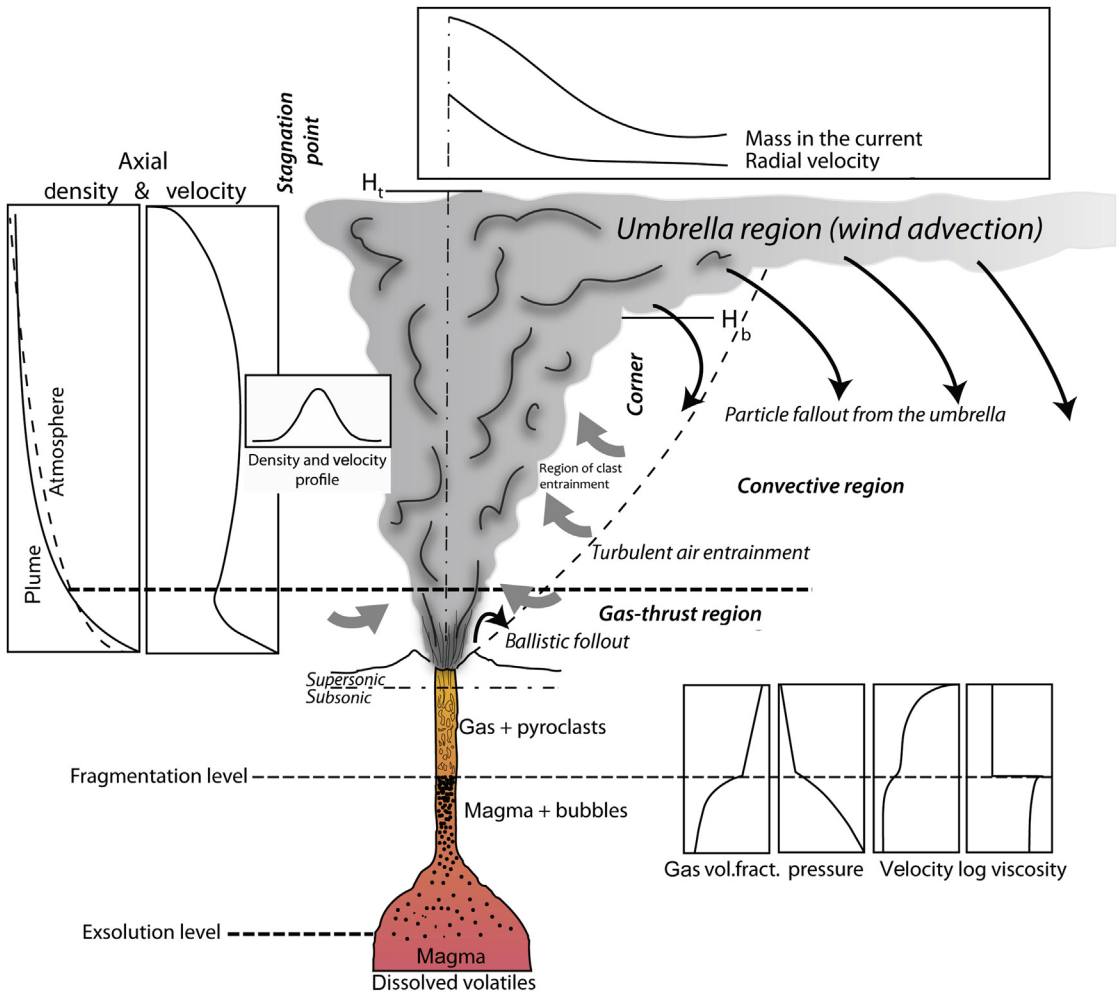

FIGURE 29.2 General scheme of eruptive regimes for a strong plume, and variation of physical parameters during plinian eruptions.

In a number of well-studied eruptions, generally described as *ignimbrite eruptions* (AD 1270 Quilotoa, Ecuador; Bronze Age Minoan, Santorini, Greece), the passage from sustained convective to collapsing column appears to be driven by progressive increase of the MDR (Figure 29.3), and marked by a gradual increase of the flow/fall ratio in the deposit sequence.

Ultraplinian eruptions differ from classical plinian events only by their higher mass flow rate, which reflects in higher columns and larger dispersal (dispersive power). The exceptionally high intensity of the ultraplinian regime, and the very large amount of fine ash generated during magma fragmentation, results in convective columns up to 55 km high (the maximum theoretical height for a convective column maintaining plume stability), which generally evolve into a collapsing column phase with the generation of high-mobility PDCs. Walker (1980) first introduced the term ultraplinian eruption, describing the fallout deposits of the AD 186 Taupo eruption (New Zealand). At present, the initial fallout phase of the 39 ka Campanian Ignimbrite eruption (Italy) is the only other described example of an ultraplinian event, suggesting that the extremely high intensity that characterizes this eruptive style could be related to the emplacement of low-aspect-ratio ignimbrites. In addition, a recent detailed study of the fallout deposits of the Taupo eruption suggests that they are better described as the superposition of the products of several powerful plinian pulses (Houghton et al., 2014).

2.2. Subplinian Eruptions

Subplinian eruptions have lower values of magnitude ($M = 4$) and intensity ($I = 10$) with respect to plinian events. Subplinian eruptions generally consist of unsteady events characterized by phases of short-period oscillations (minutes) with time breaks that can repeat several times over longer periods (days, weeks). These dynamics result in

TABLE 29.1 Main Eruptive Parameters for Plinian and Subplinian Eruptions (H_T = Column Height; MDR = Mass Discharge Rate)

Eruption	Country	Date	Composition	H_T (km)	MDR (kg/s)	Mass (kg)
El Chichon A[1]	Mexico	1982	Trachyand.	27	8.0E+07	7.5E+11
El Chichon B[1]	Mexico	1982	Trachyand.	32	1.5E+08	1.3E+12
El Chichon C[1]	Mexico	1982	Trachyand.	29	8.5E+07	1.0E+12
Santa Maria[2]	Guatemala	1902	Dacite	34	1.7E+08	2.2E+13
Mt St Helens[3]	United States	1980	Dacite	19	1.9E+07	7.1E+11
Katmai[4]	United States	1912	Rhy./Dac.	32	1.7E+08	2.5E+13
Askja[5]	Iceland	1975	Rhyolite	26	7.9E+07	8.9E+11
Vesuvius[6]	Italy	AD79	Phonolite	32	1.5E+08	6.1E+12
Santorini[7]	Greece	BC1470	Rhyolite	36	2.5E+08	3.3E+13
Tarawera[8]	New Zealand	1886	Basalt	34	1.8E+08	3.3E+13
Hatepe[9]	New Zealand	BP1820	Rhyolite	33	1.8E+08	3.8E+12
Taupo[10]	New Zealand	BP1820	Rhyolite	51	1.1E+09	7.7E+13
Tambora[11]	Indonesia	1815	Trachyand.	43	2.0E+09	2.6E+13
Etna[12]	Italy	BC122	Basalt	26	8.5E+07	9.0E+11
Hudson[13]	Chile	1991	Andesite	18	7.0E+07	2.7E+12
Krakatoa[14]	Indonesia	1883	Dacite	≈40	5.5E+08	2.9E+13
Redoubt[15]	Alaska	1989	And./Dacite	9	7.0E+06	7.5E+10
Hekla[16]	Iceland	1947	Andesite	28	4.6E+06	1.5E+12
Chaitén[17]	Chile	2008	Rhyolite	20	4.2E+07	9.6E+11
Cordon Caulle[18]	Chile	2011	Rhyodacite	14	1.5E+07	1.1E+12

[1] *Carey and Sigurdsson, 1986.*
[2] *Williams and Self, 1983.*
[3] *Carey and Sigurdsson, 1985.*
[4] *Fierstein and Hildreth, 1986.*
[5] *Sparks et al., 1981.*
[6] *Sigurdsson et al., 1985.*
[7] *Watkins et al., 1978*
[8] *Walker et al., 1984.*
[9] *Walker, 1981.*
[10] *Walker, 1980.*
[11] *Kandlbauera and Sparks, 2014.*
[12] *Coltelli et al., 1998.*
[13] *Scasso et al., 1994; Naranjo et al., 1993.*
[14] *Self, 1992.*
[15] *Miller and Chouet, 1994; Scott and McGimsey, 1994.*
[16] *Thorarinsson, 1949; Thorarinsson and Sigvaldason, 1972.*
[17] *Alfano et al., 2011.*
[18] *Bonadonna et al. (2014).*
References in supplementary material. Please see companion site, http://booksite.elsevier.com/9780123859389/

the formation of fairly short-lived convective pulses, frequently followed by the generation of small-volume PDCs. In some cases, during time breaks between subplinian pulses, episodes of lava effusion can occur. Unsteadiness (destabilization of the convective column and occurrence of time breaks) is possibly related to the decline of ejection velocity and decoupling between magma supply at depth and magma discharge at the surface (Scandone and Malone, 1985), more evident at the lower discharge rates (10^6–10^7 kg/s), typical of these eruptions. Duration of individual subplinian pulses generally varies from minutes to hours, and higher frequency fluctuations in the discharge are recorded in the resulting products as thin, alternating beds of coarser to finer-grained fallout deposits. Subplinian convective plumes generally do not cross the tropopause; in many cases the vertical velocity of the convective column is

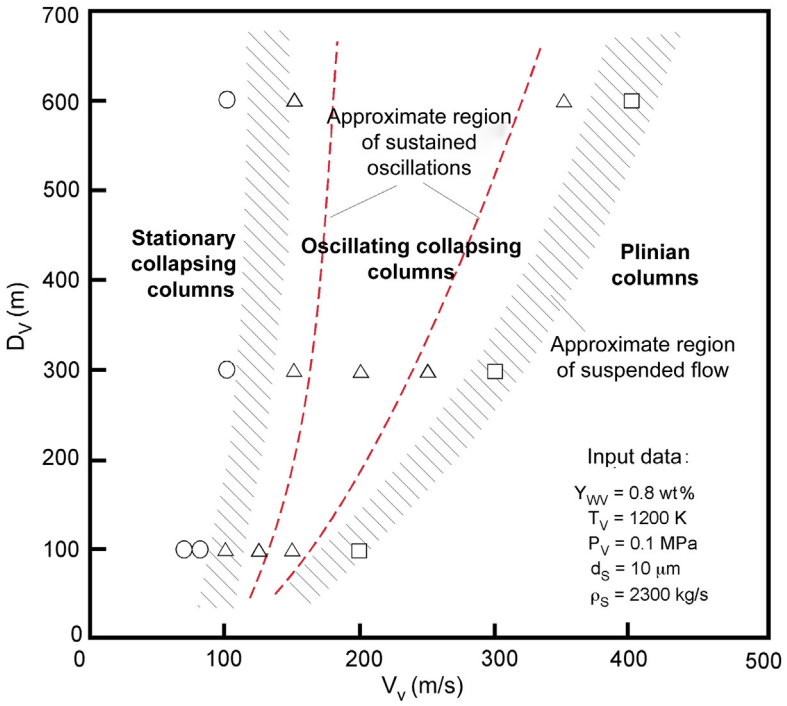

FIGURE 29.3 Relationship between the vent diameter and vent exit velocity showing different regions of volcanic columns. The cross-hatched regions identify the transition among stationary collapsing columns, oscillating columns, and plinian columns. Y_{WV} = water content, T_V = temperature, P_V = pressure, d_S = particle size, ρ_S = density. *Redrawn after Neri and Dobran (1994). References in supplementary material. Please see companion site, http://booksite.elsevier.com/9780123859389/*

moderate (weak plumes), and the plume can be noticeably bent-over in the presence of strong winds. At least five subplinian eruptions occurred at Mt St Helens in the six months after the 18 May 1980 climactic eruption; several subplinian events occurred in a period of months at Redoubt (1989–1990) and at Spurr (1992) volcanoes (Alaska). This activity was characterized by generation of sustained (although in some cases short-lived) plumes and PDCs by (partial) column collapse. In a review of past activity of Somma-Vesuvius (Italy), Cioni et al. (2008) discriminated between two different types of subplinian eruptions on the basis of the presence or absence of associated PDC deposits. In many cases, subplinian activity is gradational to violent strombolian activity in terms of characteristics of the eruptive cloud and related fallout deposits. Vulcanian explosions generating short-lived, convective ash plumes that rapidly detach from the eruptive source and are laterally advected by winds have been sometimes erroneously described as subplinian pulses.

3. THE PLUMBING SYSTEM OF PLINIAN AND SUBPLINIAN ERUPTIONS

The composition of magma driving most of plinian and subplinian eruptions is intermediate to silicic. From a compilation of 45 Pleistocene and Holocene plinian eruptions (Carey and Sigurdsson, 1989), about 80% have evolved composition (SiO_2 higher than 60 wt%). Only few basaltic plinian eruptions are known (Tarawera 1886, New Zealand; Etna 122 BC, Italy; Fontana Lapilli eruption, Masaya, Nicaragua; Figure 29.4(A)), while trachyandesitic to andesitic eruptions are more frequent (e.g. Cotopaxi, Ecuador, or Ruapehu, New Zealand). Conversely, subplinian eruptions are generally linked to intermediate magma compositions.

Magma chamber features (size and depth), as well as magma composition, may have strong influence on the dynamics of plinian eruptions. Uniform composition or vertical zoning of plinian deposits suggest that magma feeding the eruption may be tapped from homogeneous, possibly large, regional magma reservoirs (plutons), or from volumetrically smaller, compositionally stratified magma chambers. Compositionally zoned plinian deposits generally record a reversal of the magma chamber stratification, with the topmost, most evolved region of the reservoir being erupted first (Figure 29.4(B)). Despite this, the observed compositional gradient is often the result of a combination of factors such as the sequence of magma extraction from the reservoir and the occurrence of syn-eruptive mixing of different parcels of magma within the magma chamber and along the conduit. The dynamics of magma tapping and ascent, the internal gradients of the physical properties of the magma, as well as the shape of the magma chamber, control the syn-eruptive magma mixing process.

Efficient syn-eruptive magma mixing can also occur inside the magma chamber, in the course of the eruption,

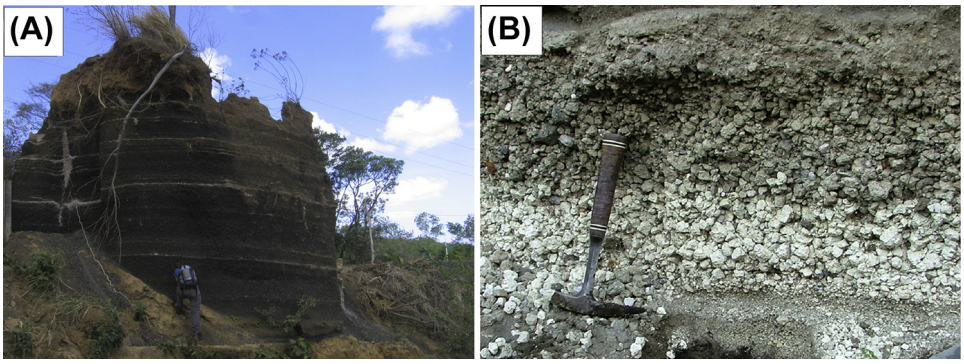

FIGURE 29.4 (A) Deposit of the basaltic plinian Fontana lapilli eruption, Masaya (Nicaragua). (B) Compositionally zoned deposit of the Bronze Age eruption of Avellino Pumice (Vesuvius, Italy). *(A) is courtesy of C. Bonadonna.*

triggered by partial emptying and local decompression of the reservoir, or by the catastrophic collapse of the magma chamber walls during caldera collapse. Physically mingled, often banded pumice clasts carrying portions of contrasting magma compositions record magma mingling that takes place shortly before the eruption. Compositional magma hybridization requires more time, and can eventually be observed in the final products of the eruption. The sudden change of magma composition during the course of an eruption can result in important changes of eruption dynamics, due to the link between magma composition, type/amount of dissolved volatiles, and the rheological and physical properties of the erupting magma. During the AD 79 Pompeii eruption of Vesuvius, the shift from phonolitic to tephriphonolitic magma composition (marked in the deposits by the passage from white to grey pumice) triggered the first partial collapse of the convective column, and favored the progressive increase of MDR mainly due to the important decrease of magma viscosity.

At several volcanoes (Novarupta, Mt St Helens, Pinatubo), the presence of deep volcano-tectonic seismicity at the end of a plinian eruption has been related to important changes of the local stress field due to the rapid removal of some cubic kilometers of magma from beneath the volcano. Such enhanced, deep fracturing possibly triggers the ascent of more mafic magma from depth, which may contribute to the final phases of degassing and eventually mixes with the unerupted magma in the reservoir, determining the ejection of a more mafic magma during the late stages of the eruption.

4. MAGMA ASCENT AND FRAGMENTATION

The depth of the magma reservoir, as estimated by petrological or geophysical methods, is used to infer the length of the conduit. If the local stratigraphy is known, then the type of accessory lithic fragments in the deposits represents an effective way to infer the lateral dimension and length of the conduit. Shea et al. (2011) used the mass of total ejected lithics to evaluate the diameter of an assumed cylindrical conduit during the AD 79 Vesuvius eruption, finding values from few meters at the beginning of the eruption to 65 m by the end of the plinian phase (corresponding to an average enlargement of the conduit radius of 1.5−2 cm/min over a conduit length of 6 km). Carey and Sigurdsson (1989) suggested a slightly higher rate of enlargement of conduit radius (around 5 cm/min) through a general analysis of 45 past plinian eruptions, in the assumption that the commonly observed increase of MDR with time is related to erosion of conduit walls. In the case of subplinian eruptions, available numerical models suggest that smaller conduit diameters (around 10−15 m) are needed.

Magma ascent during plinian eruptions can be approximated to a quasi-steady process, sustained by the pressure difference between the magma chamber and the surface, and mainly dominated by decompressional degassing. Magma degassing generally occurs under closed conditions, as a consequence of the mechanical coupling between growing vesicles and the high-viscosity magma (bubbly flow regime). However, degassing may pass from closed to open conditions if magma reaches an internal high permeability before fragmentation, and if the characteristic transit time in the conduit is long enough to allow gas release through the magma column. This process is likely to occur on a large scale in the final stages of those plinian eruptions characterized by a decrease in MDR, allowing a massive gas release, which can be responsible for long-lasting phases of ash emission and/or extrusion of viscous lava flows or lava domes. During ascent, magma density (Figure 29.2) steadily decreases as a result of decompression-driven gas exsolution and vesicle expansion; such a process contributes to the acceleration of the magmatic foam in the conduit. In contrast, magma bulk viscosity increases several orders of magnitude until the fragmentation level is reached (Figure 29.2). Available numerical models of conduit flow provide, under certain assumptions, estimates of the

continuous variation of the main parameters governing magma ascent.

High magma ascent velocities are needed to maintain the high MDR of plinian eruptions. Lateral gradients of the physical and rheological parameters in the magma likely accompany the rapid acceleration of the vesiculating magma in the conduit. Given the generally high viscosity of plinian magmas, the development of boundary layers along the conduit walls is important in reducing drag effects during magma ascent. In crystal-poor magmas, shearing along the walls results in stretching and alignment of vesicles, locally reducing the viscosity of the magma. This effect is clearly recorded in a large proportion of tube (woody) pumice in the deposits of these eruptions. In crystal-rich magmas, the high friction along the conduit walls results in crystal milling and temperature increases by viscous heating, with a consequent local decrease of the viscosity. This may promote partial crystal resorption and heterogeneities in glass composition, sometimes observed in mingled pumice clasts of large plinian eruptions (Pinatubo 1991, Philippines; Quilotoa AD 1220, Ecuador).

The decompression rate strongly controls final magma vesicularity (in terms of size and number of vesicles), and hence the style of magmatic foam fragmentation. For a conduit length of 5–8 km (the common depth range of crustal magma chambers), and MDR typical of a plinian regime, ascent times of the orders of minutes are estimated using the available numerical models, resulting in average decompression rates in the order of 1 MPa/s, and in peak decompression rates up to 10–100 MPa/s (Shea et al., 2011). Mechanisms of magma fragmentation in plinian eruptions are classically related to the reaching of a critical concentration of bubbles in the magma (about 75 vol%), or to processes of strain-rate dependent brittle fragmentation. Both processes are possible and not mutually exclusive. At high vesicle concentrations, decompressional and diffusional growth of bubbles is in part hampered by the increase of viscosity of the residual, volatile-poor liquid. Rupture of the liquid films separating gas bubbles can also occur following a progressive increase of the differential pressure, which may develop during final expansion of bubbles until the failure strength of the surrounding melt (*stress criterion*). Analog experiments have shown that explosive disintegration of the erupting foam can occur in coincidence with the highest acceleration rates in the conduit. If the timescale for deformation is shorter than the timescale for viscous relaxation of the liquid (the time needed for the liquid to keep pace with an applied strain), the bubble–liquid mixture crosses the glass transition, behaving in a brittle fashion and disintegrating (*strain criterion*). The mechanisms of fragmentation and the magma permeability play an important role in the final grain-size distribution of pyroclasts. Permeability (through bubble coalescence) will favor gas escape and consequent formation of lapilli versus ash. Delayed bubble nucleation and expansion related to disequilibrium degassing may result conversely in a very fine-grained disintegration of the magma, due to the explosion of a highly vesicular melt, characterized by a high number density of unconnected small vesicles. Comminution of fragmented magma clasts may continue during ascent in the conduit by two additional processes: (1) high-velocity particle–particle collisions, as clearly demonstrated by the experimental and theoretical analysis of Dufek et al. (2012); (2) disruption of the vesicles trapped in the glass due to the rapid decompressional gas expansion. As a consequence of these two processes, the depth of magma fragmentation may also exert an important control on the final size of the clasts.

Fragmentation acting during subplinian events reflects the unsteady character of these eruptions. The alternation of sustained columns with periods of quiescence has been explained in terms of syn-eruptive degassing and viscosity increase of the magma column during the slow ascent in the conduit. The partially degassed, high-viscosity portion of the magma crystallizes rapidly, causing magma stagnation in the upper portions of the conduit (in some cases culminating in a dome extrusion), and a progressive pressure buildup that eventually reopens the system. This process repeatedly occurred, for example at Mt St Helens, following the climactic phase of the 18 May 1980 eruption. The discontinuous nature of several subplinian eruptions is likely to be regulated by differences between the rate of magma discharge at the surface (MDR) and the rate of magma supply from the magma chamber (Magma Supply Rate, MSR). If MDR is greater than MSR, the fragmentation surface migrates downward in the conduit, until fragmentation ceases and eruption stops (Scandone and Malone, 1985). Conditions that may favor a decrease of MSR are high viscosity, increase of magma during syn-eruptive degassing, and groundmass crystallization, as well as decrease of the conduit diameter by lining of crystallizing magma. During plinian eruptions, a fully connected conduit between the reservoir and the surface may develop, allowing the sustained discharge of magma for a prolonged time, whereas during subplinian events this possibility could be hampered. Scandone et al. (2007) suggested that mid-intensity, discontinuous eruptions like subplinian events could be related to the periodic release of distinct pulses of evolved magma ("magma quanta") from a reservoir through a network of opening–closing fractures, implying an average low MSR and resulting in distinct, short phases of high discharge.

Vent geometry is fundamental in modulating the exit conditions of the eruptive mixture during high-intensity explosive eruptions. Acceleration to ultrasonic velocities and equilibration to the ambient pressure of the erupting mixture occur inside the crater and are preconditions to the formation of a vertically directed eruptive jet.

The modalities of decompression contribute to shape the crater, by erosion and land sliding of the steep, often incoherent walls, creating a feedback process that favors early pressure equilibration and sonic/supersonic transitions of the erupting mixture. Phases of vent widening are often recorded in the plinian fallout deposits as lithic-enriched beds dominated by shallow-seated wall rock fragments.

The tapping of large amounts of gas-rich magma during plinian eruptions may eventually trigger the collapse of the roof of the magma reservoir and the formation of a caldera. When caldera collapse occurs during the eruption, it modifies eruption dynamics, recompressing the residual magma in the reservoir, and causing the massive input of the host rock blocks and the contact with the magma of external fluids, favoring the onset of phreatomagmatic activity. A concurrent transition from central to fissural (ring-fault) activity may also occur. The massive incorporation of lithic fragments in the eruptive mixture during caldera collapse may in turn promote the collapse of the **eruptive plume** and the formation of PDCs.

5. ATMOSPHERIC DYNAMICS

The general physics of plinian column behavior is captured in buoyant plume theory; in no-wind or moderate wind conditions the column is roughly axisymmetric and parameters such as density and velocity of the erupting mixture are maximum along the central axis; lateral decay of these parameters can be approximated by a Gaussian function (Figure 29.2). Density and velocity also show a general upward decrease. Velocity decrease may or may not be monotonous; plumes generated by high-MDR eruptions, for example, may show significant acceleration at the passage between the gas thrust and the convective region (*superbuoyant columns*), due to efficient incorporation and heating of ambient air, or from release of latent heat from water condensation. Average vertical velocity in the ascending column controls the transport capacity of the plume as well as the distribution of the transported pyroclasts (in terms of size and density). Carey and Sparks (1986) proposed a model of the velocity field in the eruptive column in which the maximum size of the clasts that can be transported at different elevations in the convective column or in the umbrella region is related to the mass flow rate of the eruption. For this reason, the maximum size of pyroclasts found in the mid-distal fallout deposits decreases from plinian to subplinian eruptions. The diameter of the maximum lithic clasts dispersed by the umbrella region, and hence expected to be found in the deposits beyond the column corner distance (Figure 29.2) is in the order of 4–5 cm for plinian phases (for values of MDR higher on average than 10^7 kg/s), and not larger than 1–2 cm for large subplinian events (MDR between 10^6–10^7 kg/s).

The physics of the umbrella region in plinian eruptions is dominated by a centrifugal lateral intrusion into the atmosphere. Wind plays an important role by producing an elongated plume shape (and resulting fall deposits) in the downwind direction. The occurrence of westerly, large-scale meandering jet streams immediately under the tropopause at latitudes between 30° and 60° in both the hemispheres (at an altitude variable of 6–10 km and 10–16 km for the polar and the subtropical jet streams, respectively) often results in a strong lateral advection of the topmost part of the ascending plumes. In some cases, these strong winds shear the top of volcanic plumes, producing elongate tephra deposits. Due to their lower flux rates, subplinian plumes are more influenced by lateral winds in the upper troposphere, as shown by long, narrow, often asymmetric deposit dispersal.

6. PRODUCTS—DENSITY AND COMPONENTRY

During plinian eruptions, a mixture of finely fragmented multiphase magma, solid fragments of preexisting rocks and gas is injected in the atmosphere. Magma fragments (juveniles; Figure 29.5) mainly consist of highly vesicular pumice clasts and ash fragments (pumice and glass shards), along with minor amounts of variably vesicular to dense, comagmatic clasts (dense magma fragments and magma chamber-derived intrusive rocks).

Juvenile fragments forming plinian deposits generally show a narrow range in vesicularity and small textural variability (clast morphology, vesicle shape, crystal content), which contrast with the wider variability often observed in subplinian products. Bulk vesicularity of pumice clasts from plinian deposits ranges on average between 65 and 85 vol%, and it may vary along the eruption sequence due to variations in MDR and eruption dynamics. Conversely, bulk vesicularity of subplinian juvenile fragments may range from 10 up to 80 vol% within a single eruption, with multiple frequency modes between 40 and 75 vol%. The coexistence of variably vesicular fragments within the same deposit can be related to the presence of large physical gradients in the ascending magma as compared with plinian eruptions. For example, the lower MDR of subplinian eruptions likely involves narrower conduits, implicating a major role of boundary effects at the margins of the conduit, leading to lateral vesicularity gradients in magma. The simultaneous expulsion of variably vesicular magma fragments can also be related to the pulsatory nature of subplinian eruptions; rapid decompression of discrete parcels of volatile-rich magma can trigger the fragmentation of the degassed magma still residing in the conduit.

Wall-rock lithics are more abundant in plinian than in subplinian eruptions, reflecting a more effective erosion of

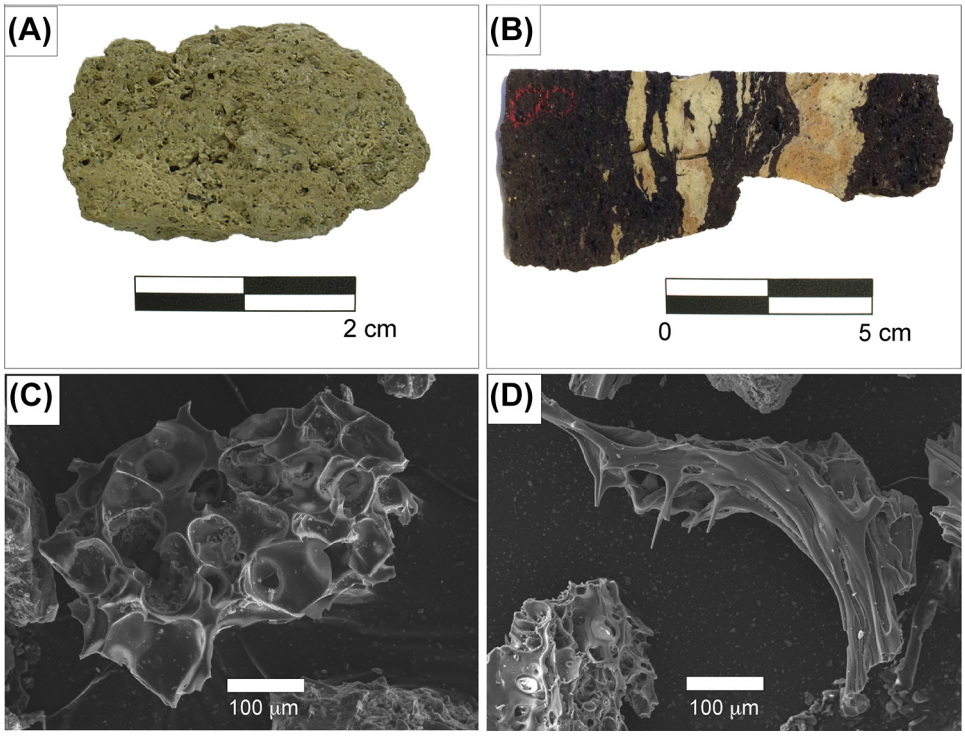

FIGURE 29.5 Variability of the juvenile component of plinian products. (A) Pumice clast. (B) Rhyolite-andesite banded pumice (1912 Novarupta-Katmai eruption, Alaska). (C) Micropumice fragment. (D) Glass shard.

the conduit/crater system. Variations in the composition and relative abundance of lithic fragments during the eruption may also provide information on the evolution, collapse, and clearing of the conduit/crater. The study of magma chamber-derived lithic fragments (such as comagmatic, salic-intrusive, mafic cumulites, thermometamorphic, or deep-hydrothermally altered rocks) may also provide clues on the position of magma chamber and hydrothermal systems. Strong increases of fragments of rocks hosting regional aquifers can also suggest phreatomagmatic activity.

7. DEPOSITS

Due to the complexity of the eruptive regimes and occurrence of multiple eruptive pulses, plinian eruption deposits typically exhibit variability in terms of types, products, dispersal and sedimentological features. A first main division for the description of the deposits can be conveniently done between fallout and flow deposits, although they can often be interlayered.

7.1. Fall Deposits

Fall deposits result from the settling on the ground of pyroclasts from the eruptive plume or the volcanic cloud, forming sheet-like layers dispersed over large areas. Due to their wide dispersal, plinian deposits represent excellent, isochronous marker beds for stratigraphic correlations; in addition, their study can be successfully used for the reconstruction of the eruptive dynamics and assessment of eruptive parameters like volume, MDR, column height, etc. **Isopach** and **isopleth** maps (Figure 29.6), as well as the study of the erupted products in terms of their grain-size, componentry, density, compositional and textural features of the **juvenile clasts**, represent fundamental steps in order to describe and quantify the eruption dynamics (Figure 29.7).

Plume dynamics and wind field at the time of eruption control tephra dispersal during plinian events (Figure 29.6(A) and (B)). Asymmetric dispersal of fallout deposits (or multilobed deposits) can be the result of variable wind directions at different altitudes during a prolonged sustained eruption characterized by a progressive change in MDR. Asymmetry in the dispersal fan can also be related to the juxtaposition of different lobes with variable dispersal, as a result of a change in wind directions during different plinian pulses. These lobes generally grade one into the other at their margins, and are often difficult to separate.

Pumice fragments are likely to break at impact especially at proximal sites, where they are coarser and often fractured by cooling contraction before landing. In contrast, lithic clasts do not break upon impact and their size in the deposit truly reflects dispersal and sedimentation processes. In distal,

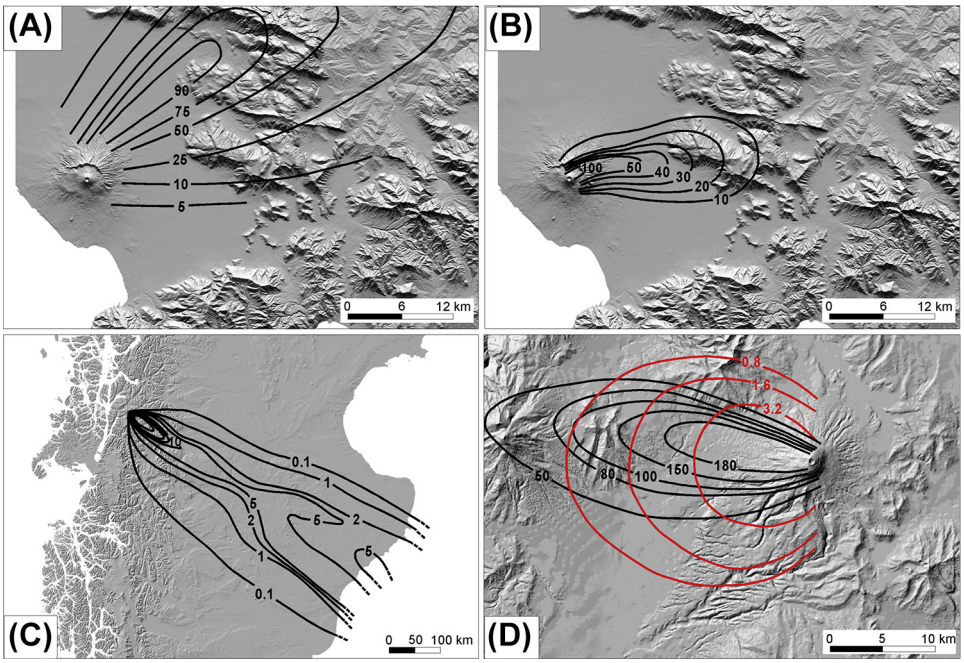

FIGURE 29.6 Isopach maps of (A) Avellino Pumice (Sulpizio et al., 2010) and (B) 1631 (Rosi et al., 1993) eruptions of Vesuvius, Italy. (C) Isopach map of the 1991 Hudson eruption, Chile (Scasso et al., 1994). Note secondary maxima in the fallout deposit. (D) Isopach (black lines; kg/m^2) and isopleth data (red lines; cm) for layer 5 at Cotopaxi volcano, Ecuador (Barberi et al., 1995). *References in supplementary material. Please see companion site, http://booksite.elsevier.com/9780123859389/*

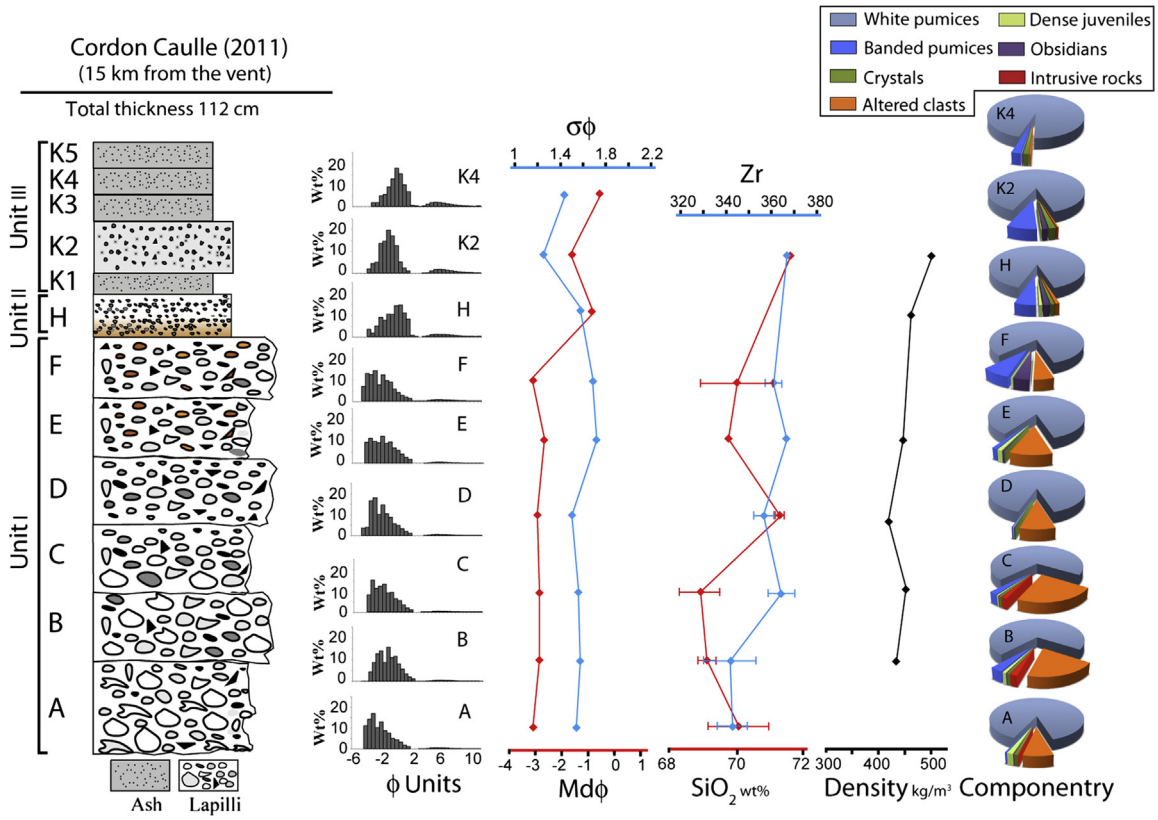

FIGURE 29.7 Stratigraphic column of the 2011 Puyehue-Córdon Caulle eruption (Chile) at 15 km east of the vent. Variations of grain-size parameters, SiO_2 and Zr content, density of pumice clasts, and componentry are also shown on the right.

ash-dominated regions of the volcanic cloud, aggregation of the airborne fine ash particles (<250 μm) frequently occurs due to electrostatic attraction or wet cohesion. This phenomenon increases the apparent terminal fall velocity of the particles. Because ash aggregation becomes effective at a certain distance (tens to hundreds km) from the vent, it may result in the formation of a secondary thickness maximum in the deposits (Figure 29.6(C)).

Grain-size distribution of samples of plinian deposits is generally polymodal (Figures 29.7 and 29.8). This is, in part, related to the fallout of clasts with different density, but roughly equivalent fall velocity. For example, large, low-density pumice clasts fall synchronously with smaller, denser lithics or crystals.

In the rare case of weak or no-wind conditions (more commonly corresponding to eruptions in the tropics, with weaker, high-level jet streams), the deposit has symmetrical dispersal around the eruptive vent. The lack of a strong asymmetry is accompanied by poor to moderate sorting of the coarse-grained deposits, and these are topped by a normally graded (fining upward) ash bed. This **co-plinian ash** is the result of the slow settling of fine particles after the end of the eruption, and is modulated only by the fall velocity of the particles (Figure 29.9(A) and (B)).

The rate of decrease of deposit thickness away from source reveals features of the eruption dynamics. These patterns can be described in a variety of ways on log thickness—area$^{1/2}$ diagrams, by multiple exponential segments, or by power laws or Weibull distributions (Pyle, 1989; Bonadonna and Houghton, 2005; Bonadonna and Costa, 2012). When tephra deposits are completely preserved on land and can be traced over long distances in a continental setting (e.g. Mt St Helens 18 May 1980; Quizapu 1932; Hudson 1992), plinian fall deposits formed in presence of wind typically show increase of thickness up to a maximum value moving away from the source vent and along the dispersal axis, followed by a slow decrease into mid-distal regions, and a secondary maximum at distal sites. The general fine-grained total grain-size distribution associated with plinian eruptions favors the efficiency of ash aggregation. Once compaction is completed, the bulk density of the deposit shows a general increase with distance, due to the combined effect of increased density with fining of the grain-size and the lower porosity of fine-grained ash beds.

Fine-grained particles injected in the stratosphere by plinian columns travel for weeks to months before settling to the ground, circumnavigating the globe several times. Most of the total ejected volume consists of fine ash dispersed over huge areas and is rarely preserved as discrete beds in continental settings, unless rapid burial protect them from erosion and remobilization. Many recent plinian events have occurred on volcanic islands or close to the coast, where most of the pyroclasts settled over the ocean. The difficulty in mapping distal deposits in oceanic settings results in major uncertainty in assessing the total erupted volumes and total grain-size distribution.

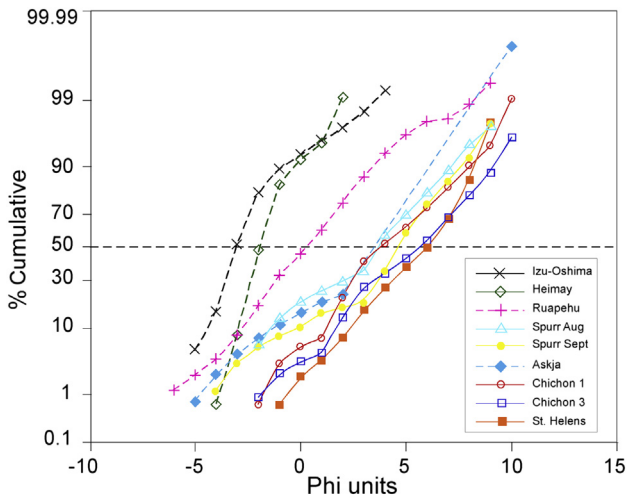

FIGURE 29.8 Total grain-size distribution of plinian and subplinian deposits, with phi $= -\log_2 D$, where D is the particle diameter in millimeters.

7.2. Proximal Deposits

Deposits within 5–10 km from the vent result from the rapid accumulation of coarse material from the gas-thrust region and from the margins of the convective column, up to the corner of the umbrella region. Due to the direct dependence of the corner position on column height, this region may range up to 20 km from the vent (Sparks, 1986). Ballistic ejecta are generally dispersed within 4–5 km of the crater; an accurate study of dispersal, shape, and size of ballistics may provide important information on exit velocity and vent position (Wilson, 1976).

Additional complexities are at work in the proximal area. For example, clasts falling from the umbrella cloud may be recycled back into the rising column by advective inflow circulation (Figure 29.2); PDCs may erode (or overthicken) proximal fall deposits by scouring (or depositing). Simultaneous sedimentation of material from different regions of the eruption column generally results in coarse-grained, thick, moderately to poorly-sorted, often lithic- and bomb-rich deposits. Preservation of these deposits varies with distance from the vent, often being very poor in the first kilometers due to the steepness of volcanic edifices, occurrence of caldera collapse, and erosion by PDCs. Very-proximal (<100–200 m from the vent) deposits are rarely preserved: Fierstein et al. (1997) interpreted an ejecta ring

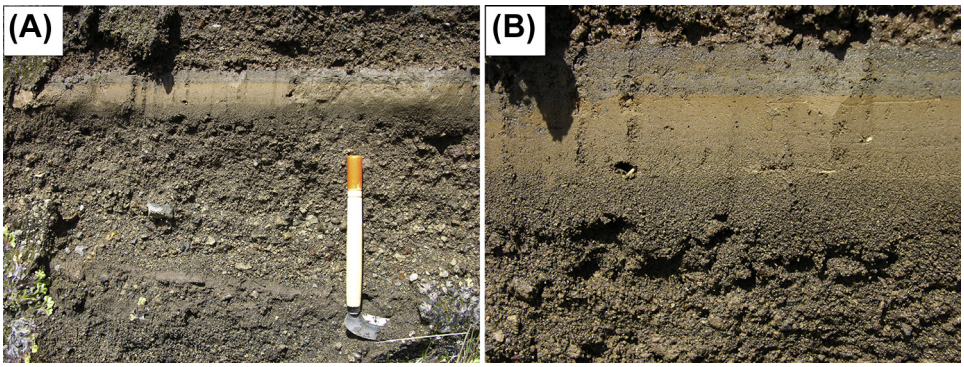

FIGURE 29.9 (A) Deposit of Layer 9, no-wind eruption of Cotopaxi volcano, Ecuador (Barberi et al., 1995). (B) Details of the Layer 9, normally graded, co-plinian ash deposit.

for the 1912 Novarupta eruption (Alaska) as the product of an irregular collar of low-fountaining ejecta encircling the main plinian plume. Welding of proximal fallout deposits related to plinian activity has been described for the Askja 1875 eruption, as well as at Cotopaxi volcano (Figure 29.10(A)).

7.3. Medial Deposits—Classification Issues

Medial deposits typically extend between 5 and 10 km and up to 40–50 km, depending on the size of the eruption and wind strength. They are generally the best preserved products and represent the classical pumice-rich, well-sorted, lapilli beds.

Medial plinian fallout deposits can be conveniently classified according to their origin process into three main categories labeled as *Simple*, *Simple-Stratified*, and *Multiple* (Rosi, 1996). This is especially useful during field surveys of proximal and medial deposits in the attempt to carry out and order all critical observations.

Simple plinian deposits result from the sedimentation of tephra from a steady eruption column. Related deposits are massive (nonstratified) or reversely graded, reflecting an increase in MDR (Figure 29.10(B)). Plinian deposits are often multiple-graded as the result of the gradual variation of the column height. Although thickness and mean grain-size decrease as a function of distance, other sedimentological features (e.g. vertical changes in the pumice/lithic ratio) do not vary with distance from vent and help to correlate among different outcrops. Due to aeolian fractionation, thinning and fining of tephra deposits away from vent can also be accompanied by changes in the relative proportions of components mainly because of the variable density of the material. Simple plinian deposits are among the most common; examples are those of Santorini Minoan (Greece), Unit five Taupo lapilli (New Zealand), and 1902 Santa Maria (Guatemala).

Simple-stratified plinian deposits commonly contain internal bedding or interlayering of PDC deposits within the fall sequence. Despite their internal stratification, these deposits are related to single eruptive events, which undergo column instability and transitions between convective and collapsing phases. Partial column collapses, particularly common during subplinian events, are frequent in this type of eruption. Reverse grading often characterizes these fall deposits; alternation of distinct tephra beds eventually grades with distance into a massive plinian fall deposit (Figure 29.10(C)). Due to their directionality, partial collapses of the eruptive column may not leave PDC deposits interbedded with the plinian fallout; in this case, they are recorded by **co-PDC ash** beds or by beds of reduced grain-size due to the temporary lowering of the eruption column. Simple-stratified deposits formed during the May 1980 eruption of Mount St. Helens and the AD 79 eruption of Vesuvius.

Multiple plinian deposits are related to separated eruptive pulses that occur in a short time interval (days to months). The rapid succession of events does not allow significant erosion or interbedding of reworked material between successive fallout beds. Individual plinian packages actually result from the juxtaposition of different tephra layers deposited under different atmospheric and eruptive conditions (Figure 29.10(D)). "Multiple" deposits can be distinguished from "simple stratified" deposits only after careful field mapping of the constituent beds, generally on the basis of dispersal axis, granulometric changes, presence of co-ignimbrite ash beds, or changes in the proportions of components. Assessment of eruptive parameters (volume and column height) demands that each single bed is studied separately in order to avoid overestimation of eruptive parameters. In very distal areas, the separation of different beds eventually becomes problematic. Eruptions with multiple plinian deposits are 1815 Tambora, 1982 El Chichón, or 2008 Chaitén. The 15 June 1991 eruption of Pinatubo (Philippine) can be also classified as a multiple plinian, as it was preceded by at least one subplinian pulse on 12 June.

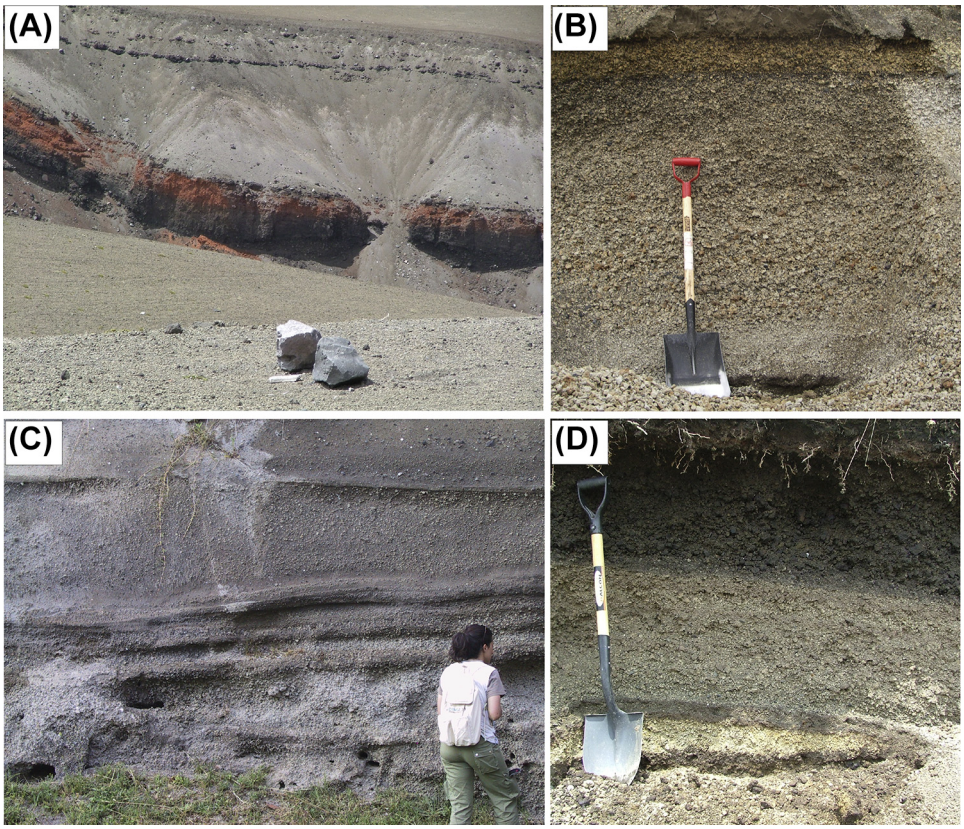

FIGURE 29.10 (A) Welded fallout deposit on the eastern sector of Cotopaxi Volcano (Ecuador). (B) Simple plinian deposit: Layer 3 eruption of Cotopaxi volcano. (C) Simple-stratified plinian deposit: the grey pumice of the AD 79 Pompeii eruption (Vesuvius, Italy). (D) Multiple plinian deposit: the layer 1 and 2 eruptions of Cotopaxi volcano.

7.4. Distal Deposits

Distal deposits of plinian eruptions (from 50 km up to several hundreds of kilometers from the source) are represented by fine lapilli to coarse ash layers that slowly thin out to millimeter-thick, fine-ash beds. Complete data sets fully describing these deposits exist only from recent eruptions. Their preservation in the geological record is, in fact, hampered by their easy reworking by wind, erosion by running water, or incorporation into the soil. Dry, fine-ash deposits are, in particular, prone to substantial wind-reworking immediately after the eruption. Fallout and sedimentation of distal ash is variably controlled by aggregation; it is common to find local thickness variations (Figure 29.6) related to differences in the aggregation efficiency in the ash cloud. Locally, preferential accumulation may be also related to the effect of low-level winds on the slowly falling material, to rapid remobilization after settling, or to differential post-depositional compaction. Due to the very low inertia when settling, ash tends in fact to form soft, uncompacted beds, which progressively compact from rain or snow. Data collected on the 1932 eruption of Quizapu (Chile) demonstrated that distal thickness nearly halved compared to data collected one year after the eruption, while this effect was insignificant for coarser, medial deposits.

7.5. Subplinian Deposits

Due to lower intensity, and hence column height, subplinian eruption clouds tend to inject less material into the stratosphere, if at all. Tephra sedimentation is thus mainly controlled by low-level, (typically) weaker winds. In addition, subplinian events also exhibit lower vertical velocities than their plinian counterparts, so that both the umbrella and the vertical regions of the eruption column are more prone to become bent-over in the presence of strong winds. All these factors are reflected in the dispersal and sedimentological features of the fall deposits, which often form strongly elongate fans that can be asymmetrical (both for thickness and grain-size) with respect to the dispersal axis, as shown by the 1980 post-climactic subplinian eruptions at Mt St Helens (Waitt et al., 1981). Subplinian eruptions often consist of multiple pulses. Tephra deposits consist of several fallout beds each characterized by its own dispersal axis, leading to

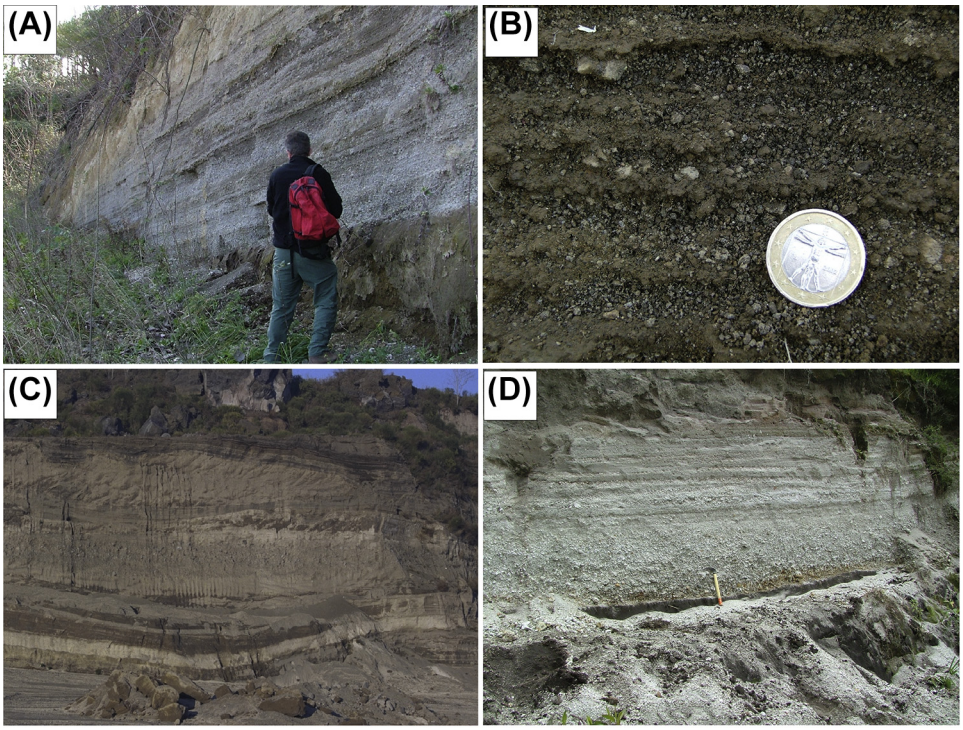

FIGURE 29.11 (A) Subplinian deposit of the Greenish Pumice eruption (Vesuvius, Italy). (B) Close view of the thinly stratified deposit of the AD 512 eruption of Vesuvius. (C) The complex proximal sequence (total thickness about 15 m) of PDC and fallout deposits of the AD 79 eruption (Vesuvius). (D) Tephra deposits of the 1.2 ka Quilotoa eruption (Ecuador); the fallout deposit of the plinian phase is overlain by a strongly stratified sequence of fallout and PDC deposits of the transitional phase of the eruption.

complex deposit architectures. These are generally thinly stratified due to grain-size alternations (Figure 29.11(A) and (B)) as seen in the recent example of the 2011 Puyehue-Córdon Caulle eruption (Chile). Compared to plinian events, subplinian deposits tend to be thinner and finer-grained at medial sites and show greater variability in the juvenile components (Figures 29.6 and 29.7).

7.6. Co-Plinian vs co-PDC Ash

Ash deposits associated with convective plinian columns are not only present at distal sites. Co-plinian, fining-upward, ash beds topping the main pumice bed have been described also at proximal-medial sites for eruptions occurring under no-wind conditions (Pululahua and Cotopaxi volcanoes; Figure 29.9). They are the result of the delayed settling of the finer-grained portion of the erupted material, which remained suspended into the umbrella region and was not widely dispersed due to the windless conditions. Conversely, co-PDC ash beds are the result of the settling of fine ash elutriated from PDCs; they may also occur interbedded in coarser, pumice-bearing tephra beds, and are generally characterized by better sorted, glass-shards-enriched, finer-grained grain-size populations. Co-PDC clouds detach from above the top of flowing PDCs with a very low vertical velocity component, allowing the elutriation of the finest particles suspended in the flow. Co-PDC fine ash beds produced by large scale pyroclastic flows can blanket vast areas.

At distal sites, co-plinian ash deposits are difficult to separate from co-PDC ash beds due to the similar size range of the two deposits; in these cases, the erroneous attribution of a co-ignimbrite ash to the plinian deposit may result in an overestimation of the total fallout volume.

7.7. PDC Activity during Plinian Eruptions

PDCs produced by the collapse of plinian columns are heterogeneous mixtures of volcanic particles and gas at high temperature, which flow across the volcano flanks driven by gravity. Although many plinian fall deposits are the result of steady- or quasi-steady state, hours-lng convective columns, steady-state conditions may rapidly shift to phases in which convection is no longer reached, leading to repeated cycles of partial or total collapses of the erupting mixture and consequent PDC generation. This dynamic is recorded in the proximal deposits as an alternation of fallout and PDC deposits (Figure 29.11(C)). When this occurs, often in response to modifications of

conduit/crater geometry, magma properties, MDR and magma fragmentation style, the erupted mass collapses back to the ground under the action of gravity, spreading as a PDC. Each time a fraction of the erupted mass is subtracted from the convective system, this results in a temporary decrease of the height of the convective column and of the dispersal of the fall deposits. Plinian eruptions commonly record repeated shifts from convective to collapsing regime, resulting in an interbedding of thin fallout and PDC beds, with the latter representing a variable, sometimes important percentage of the total erupted volume (Figure 29.11(D)).

Beyond the run-out limit attained by PDC deposits, column collapse events are recorded within the plinian fallout tephra as finer-grained beds related to the sedimentation from the lower-level, coexisting convective column, and/or by sedimentation of co-PDC ash. The presence of hybrid fallout beds consisting of centimeter-sized lapilli mixed with fine co-PDC ash accumulated synchronously also attests to the passage of the eruption through the transitional regime in which column partial collapses and sustained, buoyant phases coexist (e.g. the 1991 Pinatubo and the 1280 AD Quilotoa eruptions). In these cases, despite the increase of the total mass flow rate, the partial mass partitioning into PDCs actually results in a decrease of the height of the convective column. The coexistence of buoyant and collapsing regimes in the same eruption column may result in atypical sedimentological features of the fall deposits. If sedimentation rates of fall and PDCs are similar, poorly-sorted deposits form in which coarse and fine material coexists, sometimes showing hybrid features of fall/flow type. If sedimentation of the fallout material prevails, a poorly sorted deposit is formed, varying from a coarse bed containing an anomalous amount of ash, up to a coarse bed in which the coarse fragments are completely covered by a very fine ash patina. Conversely, if sedimentation from the PDC cloud dominates, a poorly-sorted, ash-rich flow deposit forms, bearing sparse, coarse angular fragments settled by fallout.

8. CONCLUDING REMARKS

Plinian and subplinian eruptions are very complex events consisting of different pulses of variable style, magnitude, and intensity. Although the study and modeling of the convective regime of plinian eruptions have been for decades a field of fundamental development in modern physical volcanology, much still remains to understand of the nature of these events, of the processes that control the shifts between different eruptive phases, as well as of the causes of the instabilities, which modulate subplinian dynamics. All these topics can be of utmost importance for assessing and reducing the volcanic hazards related to this type of events that, although infrequent, yet have a tremendous impact on human beings and environment.

ACKNOWLEDGMENTS

We would like to thank the many colleagues and students who, in the years, have shared with us stimulating discussions and pleasant periods in the field, and in particular Daniele Andronico, Antonella Bertagnini, Costanza Bonadonna, Kathy Cashman, Bruce Houghton, and Roberto Santacroce. The comments by Alexa Van Eaton and Simona Scollo greatly helped to improve the manuscript.

FURTHER READING

Bonadonna, C., Houghton, B.F., 2005. Total grain-size distribution and volume of tephra-fall deposits. Bull. Volcanol. 67, 441–456.

Bonadonna, C., Costa, A., 2012. Estimating the volume of tephra deposits: a new simple strategy. Geology 40, 415–418.

Carey, S., Sigurdsson, H., 1989. The intensity of plinian eruptions. Bull. Volcanol. 51, 28–40.

Carey, S., Sparks, R., 1986. Quantitative models of the fallout and dispersal of tephra from volcanic eruption columns. Bull. Volcanol. 48, 109–125.

Cioni, R., Bertagnini, A., Santacroce, R., Andronico, D., 2008. Explosive activity and eruption scenarios at Somma-Vesuvius (Italy): towards a new classification scheme. J. Volcanol. Geotherm. Res. 178, 331–346.

Dufek, J., Manga, M., Patel, A., 2012. Granular disruption during explosive volcanic eruptions. Nat. Geosci. 5, 561–564.

Fierstein, J., Houghton, B.F., Wilson, C., Hildreth, W., 1997. Complexities of plinian fall deposition at vent: an example from the 1912 Novarupta eruption (Alaska). J. Volcanol. Geotherm. Res. 76, 215–227.

Houghton, B.F., Carey, R.J., Rosenberg, M.D., 2014. The 1800a Taupo eruption: 'III wind' blows the ultraplinian type event down to Plinian. Geology 42, 459–461.

Neri, A., Di Muro, A., Rosi, M., 2002. Mass partition during collapsing and transitional columns by using numerical simulations. J. Volcanol. Geotherm. Res. 115, 1–18.

Pyle, D.M., 1989. The thickness, volume and grainsize of tephra fall deposits. Bull. Volcanol. 51, 1–15.

Pyle, D.M., 2000. Sizes of volcanic eruptions. In: Sigurdsson, H., et al. (Eds.), Encyclopedia of Volcanoes. Academic Press, pp. 263–269.

Rosi, M., 1996. Quantitative reconstruction of recent volcanic activity: a contribution to forecasting of future eruptions. In: Monitoring and Mitigation of Volcano Hazards. Springer, Berlin Heidelberg, pp. 631–674.

Scandone, R., Malone, S.D., 1985. Magma supply, magma discharge and readjustment of the feeding system of Mount St. Helens during 1980. J. Volcanol. Geotherm. Res. 23, 239–262.

Scandone, R., Cashman, K.V., Malone, S.D., 2007. Magma supply, magma ascent and the style of volcanic eruptions. Earth Planet. Sci. Lett. 253, 513–529.

Shea, T., Gurioli, L., Houghton, B.F., Cioni, R., Cashman, K.V., 2011. Column collapse and generation of pyroclastic density currents during the A.D. 79 eruption of Vesuvius: the role of pyroclast density. Geology 39, 695–698.

Sparks, R., 1986. The dimensions and dynamics of volcanic eruption columns. Bull. Volcanol. 48, 3–15.

Waitt Jr., R.B., Hansen, V.L., Sarna-Wojcicki, A.M., Wood, S.H., 1981. Proximal air-fall deposits of eruptions between May 24 and August 7, 1980. Stratigraphy and field sedimentology. The 1980 eruptions of Mount St Helens, Washington. In: Lipman, P.W., Mullineaux, D.R. (Eds.), Geological Survey Professional Paper 1250, pp. 601–616.

Walker, G., 1981. Plinian eruptions and their products. Bull. Volcanol. 44, 223–240.

Walker, G.P., 1973. Explosive volcanic eruptions—a new classification scheme. Geol. Rund. 62, 431–446.

Walker, G.P.L., 1980. The Taupo pumice: product of the most powerful known (ultraplinian) eruption? J. Volcanol. Geotherm. Res. 8 (1), 69–94.

Wilson, L., 1976. Explosive volcanic eruptions–III. Plinian eruption columns. Geophys. J. R. Astron. Soc. 1, 543–556.